Available online at www.sciencedirect.com

ScienceDirect

Ceramics International 40 (2014) 3341–3346

CERAMICS INTERNATIONAL

www.elsevier.com/locate/ceramint

Preparation and corrosion assessment of electrodeposited Ni–SiC composite thin films

Chunyang Ma[a], Guiqiang Liang[b], Yongyong Zhu[c], Haiwei Mu[d], Fafeng Xia[a,*]

[a]School of Mechanical Science and Engineering, Northeast Petroleum University, Daqing 163318, PR China
[b]School of Electrical Engineering, Binzhou Polytechnic, Binzhou 256600, PR China
[c]Department of Economics and Business Administration, Chongqing University of Education, Chongqing 400067, PR China
[d]School of Electronic Science, Northeast Petroleum University, Daqing 163318, PR China

Received 16 August 2013; received in revised form 22 September 2013; accepted 23 September 2013
Available online 30 September 2013

Abstract

Ni–SiC composite thin films were successfully prepared via direct-current (DC) and ultrasonic pulse-current (UPC) deposition. The morphologies, mechanical properties, and corrosion properties of the films were investigated via atomic force microscopy, X-ray diffraction (XRD), Vickers hardness test, scanning electron microscope (SEM), cyclic polarization, and gravimetric analysis. The results show that the Ni–SiC composite thin films synthesized via UPC deposition possess a compact and exiguous surface morphology. The XRD results indicate that the average grain diameters of Ni and SiC in the UPC-deposited thin film are 63.6 and 38.5 nm, respectively. The maximum microhardness values for the DC- and UPC-deposited Ni–SiC composite thin films prepared are 871.7 and 924.3 HV, respectively. In the corrosion tests, the UPC-deposited films have a higher corrosion resistance than those prepared by DC deposition with the same SiC content.

Keywords: A. Preparation; C. Corrosion; C. Ni–SiC composite thin film

1. Introduction

SiC, which is highly known as a metal carbide ceramic material, has been used in numerous applications because of its superior physical and chemical properties. Nanosized SiC particles are generally introduced into Ni-based composite thin films to enhance properties such as corrosion resistance, wear resistance, and microhardness. Given the superiority of both traditional composite materials and modern nanomaterials, Ni–SiC composite thin films have become the focus of numerous studies [1–4]. Electrodeposition is generally a simple and inexpensive method of fabricating composite thin films in a metal matrix. Recent studies on the electrodeposition of Ni–SiC composite thin films have been reported [5–8]. Gyftou et al. [9] prepared Ni matrix composite thin films containing micro- and nanosized SiC particles from an additive-free Watts-type solution at direct-current (DC) and pulse-current (PC) conditions. The study showed that the presence of SiC particles affects the adsorption and desorption around the catholyte area during electrocrystallization. Lin et al. [10] electroplated Ni–SiC composite thin films from a nickel sulfamate solution with a SiC suspension with and without the addition of monovalent Tl ions. The Tl ions absorbed on the SiC particles either modify the adsorption isotherms of the Ni ions and protons or function as a catalyst for Ni ion reduction, which provide additional nucleation sites for the electrocrystallization of equiaxed Ni grains. Narasimman et al. [11] obtained the electroplating parameters for preparing Ni–SiC composite thin films by sediment electrocodeposition. Pavlatou et al. [12] synthesized Ni matrix composite coatings containing micro- and nano-SiC particles from an additive-free Watts-type bath at DC and PC conditions. Furthermore, the effect of Ni/nano-SiC composite particle size on hardness was the strongest. A study has shown that the properties of composite thin films mainly depend on both the matrix phases and the amount and distribution of codeposited particles. In turn, these factors are related to

*Corresponding author. Tel./fax: +86 459 6507757.
E-mail address: xia331@126.com (F. Xia).

0272-8842/$ - see front matter
http://dx.doi.org/10.1016/j.ceramint.2013.09.100

numerous process parameters, including particle characteristics (particle shape, size, and concentration in solution), electrolyte composition (electrolyte concentration, additives, wetting agent, surfactant, and concentration) and applied current (DC, PC, and current density).

Ultrasound, which has a frequency of 16–200 kHz, has been applied in the medical, electroplating, and military fields, among others [13–15]. Ultrasonic dispersion is used in the preparation of composite thin films during electrodeposition. Ultrasonic electrodeposition, which involves electronic agitation to suspend particles in an electrolyte, is more effective than mechanical or magnetic stirring but is strongly affected by plating parameters such as ultrasonic power, particle concentration, current density, on-duty ratio, and bath temperature.

Despite numerous investigations on metal DC or PC deposition, reports on the application of ultrasonic PC (UPC) deposition for Ni–SiC composite thin film fabrication are few. Our recent work indicated that Ni–SiC composite thin films with superior properties could be prepared by UPC deposition. In this study, two types of Ni–SiC composite thin films were produced via DC and UPC deposition. The surface morphology and microstructure of the Ni–SiC composite thin films are discussed. The mechanical and corrosion properties of the films were also investigated.

2. Experiments

2.1. Electrolyte composition and plating conditions

Ni–SiC composite thin films with a thickness of ~50 μm were deposited on 15 mm × 10 mm × 2 mm mild steel substrates via DC and UPC deposition. And the thickness of the thin films was measured by an ultrasonic thickness detector. The mild steel substrates were used as cathodes. A schematic diagram of the basic electrodeposition cell is shown in Fig. 1. Prior to deposition, the substrates were mechanically polished to a 0.10 μm to 0.20 μm surface finish, sequentially cleaned to remove surface contamination, activated for 10 s in a mixed acidic bath, and then rinsed with distilled water and ethylic alcohol. A pure Ni (99%) plate with similar dimensions was used as the anode. To obtain electrodeposited Ni–SiC composite thin films, the electrolyte composition was as follows: 280 g/l nickel sulfate, 36 g/l nickel chloride, 30 g/l boric acid, and 1 g/l to 10 g/l SiC particles. The temperature was kept at 48 °C, and the pH was adjusted to 4.5–5.5 by using ammonium hydroxide or dilute sulfuric acid. During electrodeposition, ~30 nm SiC particles were introduced into the electrolyte at various ratios. The plating parameters for Ni–SiC composite thin film electrodeposition are shown in Table 1.

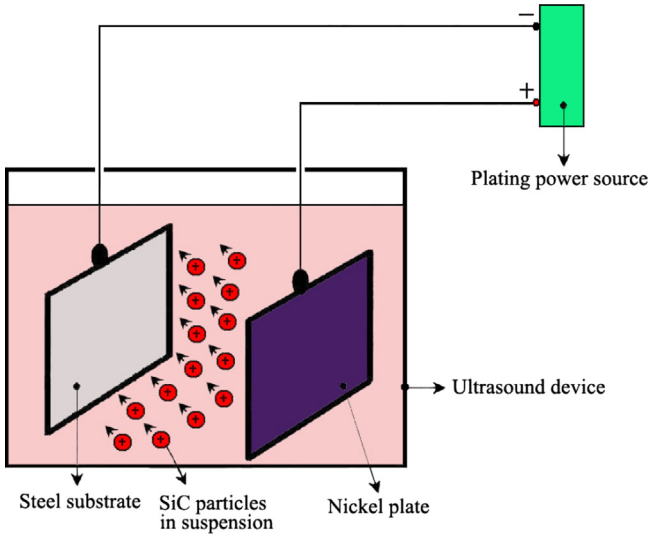

Fig. 1. Schematic diagram of the electrodeposition cell.

Table 1
The plating parameters.

Direct current deposition	
Ultrasonic power (W)	0
Current density (A/dm^2)	5
Electroplating time (min)	60
Ultrasonic pulse current deposition	
Ultrasonic power (W)	300
Current density (A/dm^2)	5
Duty cycle	0.5
Electroplating time (min)	60

2.2. Microstructural characterization

The surface morphologies of the Ni–SiC composite thin films were determined via scanning electron microscope (SEM, JEOL, JSM-6460LV) with energy dispersive X-ray analysis (EDS) and atomic force microscopy (AFM, DI, Nanoscope IIIa). The X-ray diffraction (XRD) patterns of the Ni–SiC composite thin films were obtained on a Philips D5000 instrument using Cu Kα radiation (λ=0.15418 nm). The operating target voltage was 40 kV, and the tube current was 100 mA. The Scherrer equation was used to obtain the average grain diameter as follows:

$$D = \frac{180K\lambda}{\pi\sqrt{\beta^2 - \omega\ \cos\ \theta}} \quad (1)$$

where K is the figure factor of the grains (K=0.89), λ is the wavelength, β is the width of the diffraction peak at half height, ω is the standard full width at half maximum (FWHM) and θ is the Bragg angle.

Vickers hardness was measured using a 401 MVT microhardness tester at 100 gf loads for 10 s. The SiC particle content in the composite thin films (denoted as V_p) was determined via gravimetric analysis (HIDEN, IGA-003).

2.3. Immersion test

Immersion corrosion tests were performed on the Ni–SiC composite thin films by immersing the samples in a 5 wt% NaCl solution for 180 h at 30 °C, rinsing with distilled water, and then drying in a drying oven (CIXI, FY-DR-1). Weight

loss was measured on an electronic analytical balance (SARTORIUS, BS210S) with an accuracy of 0.01 mg.

2.4. Electrochemical test

Corrosion studies were conducted using cyclic polarization (CP). After deposition, the specimens were washed in distilled water, dried in air, and then mounted in polyester to obtain an insulated surface area of 1 cm^2 for use as the working electrode. A saturated calomel electrode (SCE) ending in a lugging capillary was used to measure the electrode potential without IR drops. The auxiliary electrode was smooth platinum. CP tests were performed on the Ni–SiC composite thin films in an aerated 3.5 wt% NaCl solution at ambient temperature by using a CHI 650B electrochemical station at a scan rate of 0.2 mV/s. All experiments were conducted after the steady-state corrosion potential was attained approximately 1 h after immersion in the solution. A Pentium 4 computer and Autolab software were used to process the data.

3. Results and discussion

3.1. Morphology and microstructure

Fig. 2 shows the AFM surface morphologies of the DC and UPC-deposited Ni–SiC composite thin films. The experimental results show that the UPC-deposited Ni–SiC composite thin film displays a compact and exiguous surface morphology, whereas the DC-deposited specimen appears relatively coarse and shows irregular crystalline grain structures as a result of ultrasonication and PC, which can inhibit normal Ni crystal growth and disrupt the formation of smaller nuclei by larger crystals. Moreover, moderate ultrasonication leads to a homogeneous dispersion of SiC particles in the films. Therefore, smaller grains can be formed under the application of ultrasonication and PC. This finding indicates that the UPC-deposited Ni–SiC composite thin film is optimal, whereas the film obtained by DC deposition is relatively inferior.

The XRD patterns of the Ni–SiC composite thin films were obtained to confirm further the presence of SiC particles. Scans were recorded in the $2\theta = 30–80^\circ$ range at a scan rate of 0.02°. The XRD patterns (Fig. 3) show that the composite thin films consist of an Ni phase and a SiC phase. For Ni, the diffraction peaks at 44.8°, 52.2°, and 76.8° correspond to (1 1 1), (2 0 0), and (2 2 0), respectively. For SiC, the diffraction peaks at 34.2°, 41.6°, and 59.7° correspond to (1 0 0), (1 1 1), and (2 2 0), respectively. The average Ni and SiC grain sizes can be calculated using Eq. (1) based on the XRD data. The average grain diameters of Ni and SiC in the UPC-deposited composite thin film are 63.6 and 38.5 nm, respectively, whereas those in the DC-deposited film are 192.8 and 107.4 nm, respectively. These results are consistent with the AFM findings.

3.2. Mechanical properties of Ni–SiC composite thin films

Fig. 4 shows the effect of V_p on the microhardness of the Ni–SiC composite thin films. The microhardness slightly increases when V_p is increased from 1 wt% to 4 wt% but significantly increases when V_p is increased from 4 wt% to 10 wt%. The maximum microhardness values for the DC- and UPC-deposited Ni–SiC composite thin films are 871.7 and 924.3 HV, respectively. The improved microhardness of the films is related to the dispersion hardening effect of the SiC particles, which exhibit higher microhardness and enhance the properties of Ni–SiC composite thin films. In addition, the SiC particles embedded in the films increases the flow rate by obstructing dislocations. This trend is similar to that reported by Ashassi-Sorkhabi et al. [16].

3.3. Corrosion of Ni–SiC composite thin films

Fig. 5 shows the weight loss curves of the Ni–SiC composite thin films after corrosion. The V_p values of the composite thin films are approximately 2, 4, and 6 wt%. The corrosion weight losses of the composite thin films evidently

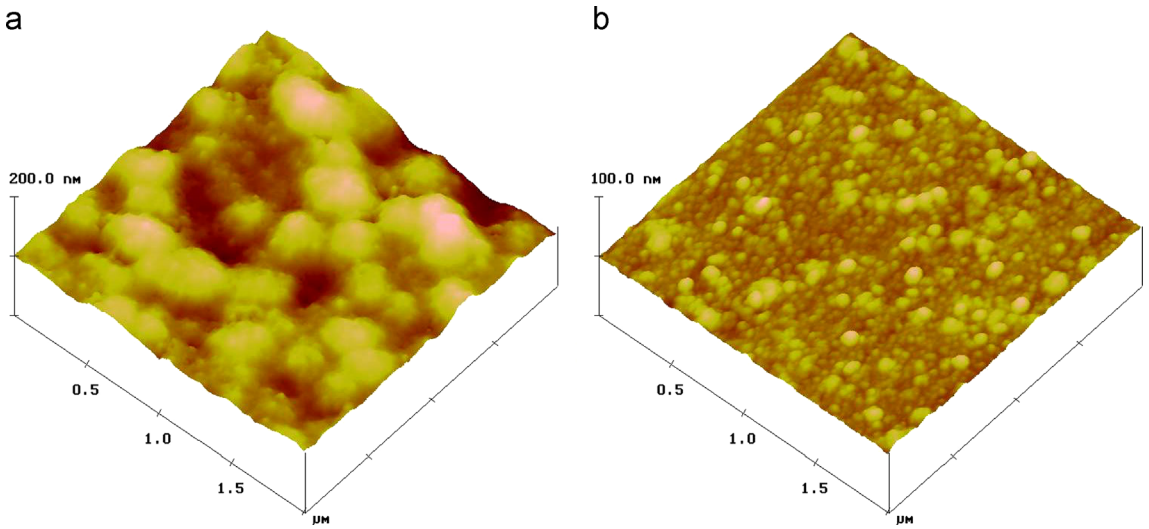

Fig. 2. AFM images of Ni–SiC composite thin films deposited by (a) DC and (b) UPC methods.

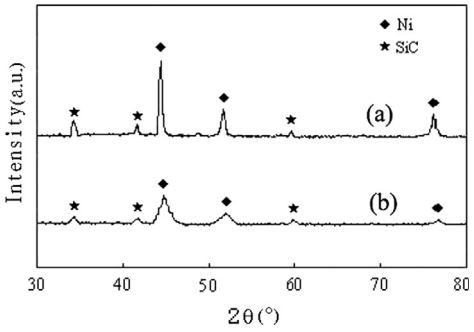

Fig. 3. XRD patterns of Ni–SiC composite thin films deposited by (a) DC and (b) UPC methods.

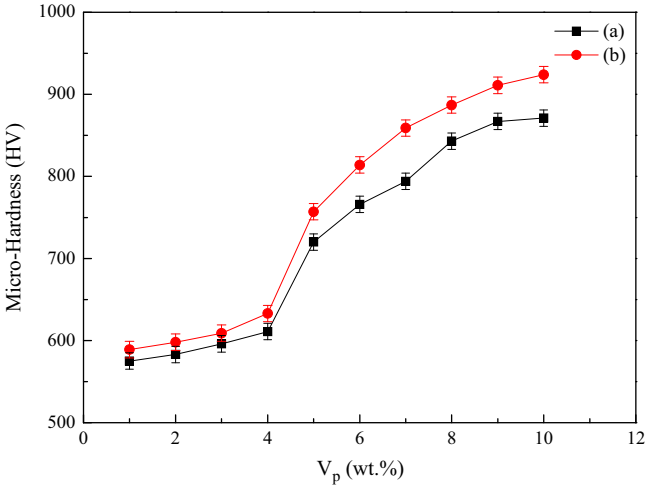

Fig. 4. The effect of V_p on micro-hardness of Ni–SiC composite thin films deposited by (a) DC and (b) UPC methods.

decrease with increasing SiC content. The trends of the corrosion curves of the DC- and UPC-prepared films are essentially the same: the curves rapidly increase initially and then gradually change. The three UPC-deposited films exhibit small weight losses, whereas the DC-deposited specimens show higher losses at similar SiC particle contents. This finding shows that the UPC-deposited Ni–SiC composite thin films have a higher corrosion resistance than the DC-deposited specimens at the same SiC content because of moderate ultrasonication, which is conducive to the homogeneous dispersion of SiC particles in the Ni–SiC composites. Moreover, the SiC particles embedded in the composite thin films increase the compactness of the films and enhance their corrosion resistance.

3.4. Corrosion morphology of Ni–SiC composite thin films

The surface morphologies of the Ni–SiC composite thin films (V_p=4 wt%) after corrosion tests for 180 h are presented in Fig. 6. The UPC-deposited film consists of regular and compact oxides with uniform and fine grains, whereas the DC-deposited specimen consists of coarse, loosely structured oxides. Fig. 6(b) shows that after immersion in 5 wt% NaCl solution for 180 h, only a few small pits appear on the surface.

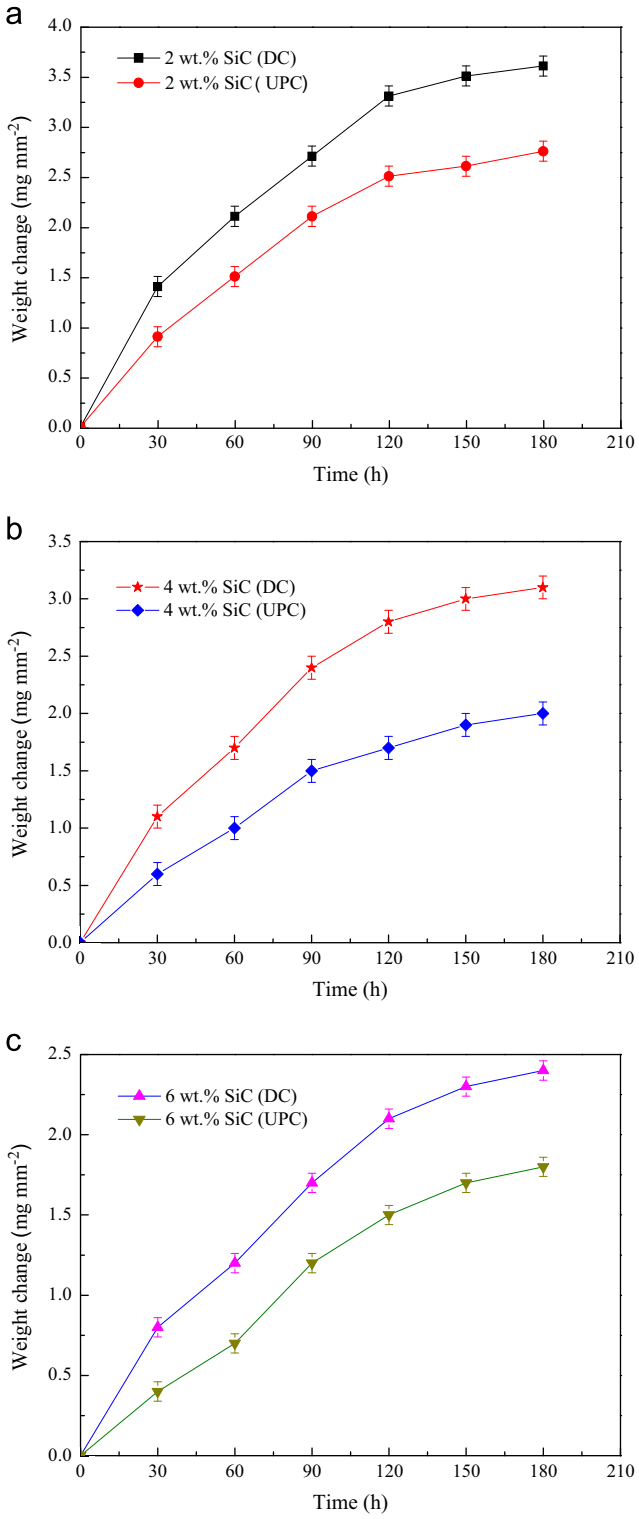

Fig. 5. Weight loss curves of Ni–SiC composite thin films after corrosion: (a) $V_p \approx 2$ wt%, (b) $V_p \approx 4$ wt% and (c) $V_p \approx 6$ wt%.

However, the DC-deposited film shows the most severe damage [Fig. 6(a)]. The EDS results (Fig. 6) also clearly show that the major corrosion products of the Ni–SiC composite thin films are NiO and $NiCl_2$. Based on the corrosion results, the corrosion mechanism of the Ni–SiC composite thin films can be explained as follows: first, the Ni atoms of the

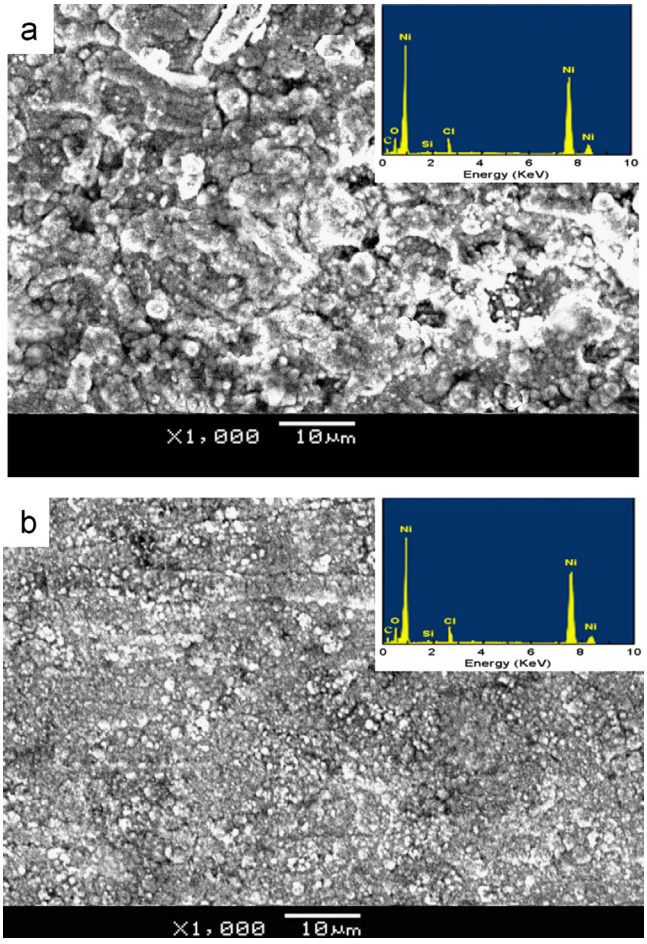

Fig. 6. SEM and EDS images of samples after the corrosion test: (a) DC and (b) UPC.

composite thin films are oxidized to NiO ($2Ni+O_2=2NiO$) and form an oxide layer. Second, the NaCl molecules on the films react with NiO to form $NiCl_2$ ($NiO+2Cl^-=NiCl_2+O^{2-}$), which can be eventually decomposed into Cl_2 ($NiCl_2=Ni^++2Cl^-$, $2Cl^-+2e=Cl_2$). Consequently, the Ni–SiC composite thin films are destroyed, and a larger number of point defects are formed. The loose oxide layer is poorly adhered to the matrix and thus fails to provide effective protection, which in turn results in the accelerated corrosion rate of the films. As the corrosion test proceeds, the oxide layer gradually thickens and eventually inhibits the corrosion reaction. This phenomenon explains the tendency of the corrosion dynamic curves to level off when the corrosion reaches a specific period.

3.5. Potentiodynamic polarization of Ni–SiC composite thin films

Fig. 7 shows the potentiodynamic polarization curves of the Ni–SiC composite thin films ($V_p=4$ wt%) in a 3.5 wt% NaCl solution. The electrochemical corrosion parameters obtained from the polarization curves are listed in Table 2. The results in Fig. 7 and Table 2 indicate that the corrosion potentials of the DC- and UPC-deposited films are −0.213 and −0.171 V vs. SCE, respectively. Moreover, the corrosion current density

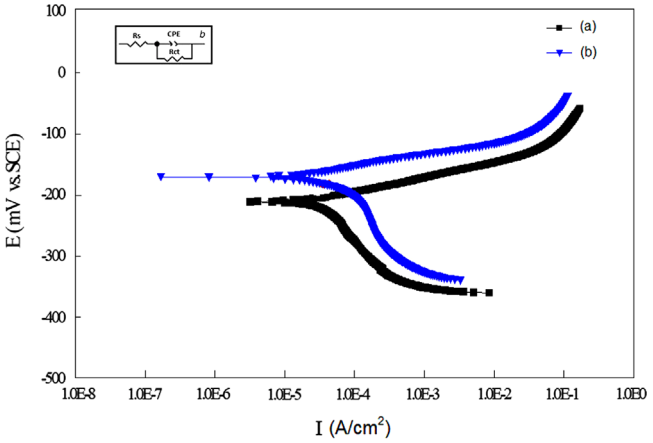

Fig. 7. Potentiodynamic polarization of Ni–SiC composite thin films deposited by (a) DC and (b) UPC methods.

Table 2
Corrosion characteristics of Ni–SiC composite thin films in 3.5 wt% NaCl solution.

Types of films	(a) DC	(b) UPC
β_a (V/dec)	0.03	0.01
β_c (V/dec)	0.02	0.02
R (Ω/cm^2)	2635	6652
E (V) vs. SCE	−0.213	−0.171
I (A/cm^2)	3.78×10^{-5}	1.07×10^{-5}

of the UPC-prepared film is 1.07×10^{-5} A/cm^2, which is lower than that of the DC-deposited specimen. This result indicates that the UPC-prepared film has higher corrosion resistance than the DC-deposited specimen, as previously shown by the SEM results.

4. Conclusions

Ni–SiC composite thin films were produced via DC and UPC deposition. The AFM results demonstrate that compared with DC deposition, Ni–SiC composite thin films with compact and fine grain sizes can be obtained via UPC deposition. The maximum microhardness values for the DC- and UPC-deposited films are 871.7 and 924.3 HV, respectively. The XRD results indicate that the average Ni and SiC grain diameters in the UPC-deposited thin film are 63.6 and 38.5 nm, respectively. In the corrosion tests, the UPC-fabricated films exhibit a higher corrosion resistance than those prepared by DC deposition at the same SiC content.

Acknowledgments

This work has been supported by the Natural Science Foundation of China (Grant nos. 51101027, 51374072), Program for New Century Excellent Talents in Heilongjiang Provincial University (Grant no. 1253-NCET-002), Foundation of Heilongjiang Province for Returned Scholars, Foundation for University Key Teacher

of Heilongjiang Province of China (Grant nos. 1251G004, 1252G008).

References

[1] Y. Zhou, H. Zhang, B. Qian, Friction and wear properties of the co-deposited Ni–SiC nanocomposite coating, Applied Surface Science 253 (20) (2007) 8335–8339.
[2] S. Xie, X.L. Tong, G.Q. Jin, Y. Qin, X.Y. Guo, CNT–Ni/SiC hierarchical nanostructures: preparation and their application in electrocatalytic oxidation of methanol, Journal of Materials Chemistry A 1 (2013) 2104–2109.
[3] D. Erogluz, A.C. West, Mathematical modeling of Ni/SiC co-deposition in the presence of a cationic dispersant, Journal of the Electrochemical Society 160 (9) (2013) D354–D360.
[4] H.M. Zheng, X.M. Huang, S.Z. He, P. Li, M. Yang, Effects of SiC particles on properties of Ni–W–P–SiC composite coatings, Metallic Functional Materials 17 (6) (2010) 49–54 (in Chinese).
[5] Z. Wu, B. Shen, L. Liu, Effect of α-Al_2O_3 coatings on the interface of Ni/SiC composites prepared by electrodeposition, Surface and Coatings Technology 206 (14) (2012) 3173–3178.
[6] P. Ari-Gur, J. Sarielb, S. Vemuganti, Residual stresses and texture in Ni/SiC nanocomposite coatings, Journal of Alloys and Compounds 434–435 (2007) 704–706.
[7] C.Y. Tan, Y. Liu, X.S. Zhao, Z.Q. Zheng, Nickel co-deposition with SiC particles at initial stage, Transactions of Nonferrous Metals Society of China 18 (5) (2008) 1128–1133.
[8] Y. Wang, H.B. Xu, Preparation and numerical simulation of Ni–SiC composite coatings deposited by electrode position, Research Journal of Applied Sciences, Engineering and Technology 5 (24) (2013) 5602–5607.
[9] P. Gyftou, M. Stroumbouli, E.A. Pavlatou, P. Asimidis, N. Spyrellis, Tribological study of Ni matrix composite coatings containing nano- and micron-SiC particles, Electrochimica Acta 50 (2005) 4544–4550.
[10] C.S. Lin, K.C. Huang, Codeposition and microstructure of Nickel–SiC composite coating electrodeposited from sulphamate bath, Journal of Applied Electrochemistry 34 (2004) 1013–1019.
[11] P. Narasimman, M. Pushpavanama, V.M. Periasamy, Effect of surfactants on the electrodeposition of Ni–SiC composites, Portugaliae Electrochimica Acta 30 (1) (2012) 1–14.
[12] E.A. Pavlatou, M. Stroumbouli, P. Gyftou, N. Spyrellis, Hardening effect induced by incorporation of SiC particles in nickel electrodeposits, Journal of Applied Electrochemistry 36 (2006) 385–394.
[13] F.F. Xia, C. Liu, F. Wang, M.H. Wu, J.D. Wang, H.L. Fu, J.X. Wang, Preparation and characterization of nano Ni–TiN coatings deposited by ultrasonic electrodeposition, Journal of Alloys and Compounds 490 (2010) 431–434.
[14] L. Zhao, Y.T. Zhan, J.L. Rutkowski, G.Z. Feuerstein, X.K. Wang, Correlation between 2- and 3-dimensional assessment of tumor volume and vascular density by ultrasonography in a transgenic mouse model of mammary carcinoma, Journal of Ultrasound in Medicine 29 (4) (2010) 587–595.
[15] F.F. Xia, C. Liu, C.H. Ma, D.Q. Chu, L. Miao, Preparation and corrosion behavior of electrodeposited Ni–TiN composite coatings, International Journal of Refractory Metals and Hard Materials 35 (2012) 295–299.
[16] H. Ashassi-Sorkhabi, S.H. Rafizadeh, Effect of coating time and heat treatment on structures and corrosion characteristics of electroless Ni–P alloy deposits, Surface and Coatings Technology 176 (2004) 318–326.